Path following for autonomous vehicle navigation with inherent safety and dynamics margin

Conference Paper · July 2008

DOI: 10.1109/IVS.2008.4621276 · Source: IEEE Xplore

3 authors:

Kristijan Macek
Varian Medical Systems
32 PUBLICATIONS **449** CITATIONS

SEE PROFILE

Roland Philippsen
Halmstad University
48 PUBLICATIONS **1,069** CITATIONS

SEE PROFILE

Roland Siegwart
ETH Zurich
798 PUBLICATIONS **38,546** CITATIONS

SEE PROFILE

Path Following for Autonomous Vehicle Navigation with Inherent Safety and Dynamics Margin

Kristijan Maček*, Roland Philippsen†, Roland Siegwart*

*Swiss Federal Institute of Technology Zurich, Switzerland
email: {kristijan.macek, rsiegwart}@mavt.ethz.ch

† Robotics Laboratory, Computer Science Department, Stanford University
email: roland.philippsen@gmx.net

***Abstract*— This paper addresses the path following problem for autonomous Ackermann-like vehicle navigation. A control strategy that takes into account both kinodynamic and configuration space constraints of the vehicle, denoted as Traversability-Anchored Dynamic Path Following (TADPF) controller is presented. It ensures secure vehicle commands in presence of obstacles, based on traversability information given by a global navigation function. By additionally using a reference point on the global smooth path, the local vicinity path configuration with respect to the vehicle is taken explicitly into account to ensure smooth and stable path following. Furthermore, a previously developed Sliding Mode Path Following (SMPF) controller that results in fast convergence rate and low path following error but which does not consider kinodynamic constraints, is augmented by the the kinodynamic and configuration space constraints check of the TADPF controller. The new proposed control strategy denoted as TADPF-SMPF controller thus combines advantageous characteristics of both original control strategies for path following, yielding inherent safety and vehicle dynamics margin. All three control strategies are verified in simulation, whereas the TADPF and TADPF-SMPF path following schemes are also verified experimentally.**

I. Introduction

In order to achieve a goal objective a deliberate planning phase is needed in any autonomous vehicle navigation sheme. Assuming the planning is performed in configuration space, its result can be described as a geometric path (whether holonomic or non-holonomic). The intermediate execution layer connecting such a reference geometric path (not parametrized in time) and the low-level vehicle control is solved by path following, which was notably studied in [1] using a pure pursuit algorithm, exponential control law in [2], a chained form approach in [3], optimal trajectory generation in [4], small-time controllability scheme in [5] and robust feedback-linearization in [6] among others. Whereas many different feasibility aspects were successfully studied and solved, very few approaches considered both the case of a changing reference path due to the frequent replanning needed in unknown/changing environments and taking into account kinematic and dynamic vehicle constraints while following the path.

This paper aims at such an integration, where three distinctive path following strategies for global vehicle navigation are analyzed. It assumes existence of a navigation function that generates an on-line path towards a global objective and optionally also generates traversability cost estimates for changing environments with limited vehicle's sensor range, such as $E^\star$ ([7]) or Field-$D^\star$ ([8]). A reference point path following technique by the authors was first presented in [9]. The follow-up TADPF controller was presented in [10] and modified here to account for driving comfort based on lateral acceleration constraints of the vehicle, which affects primarily the longitudinal velocity profile of the vehicle. A comparison is made on the path following precision and steering control effort with the SMPF controller presented in [11]. A novel combination of the TADPF controller and the SMPF controller for path following is proposed which enables collision-free navigation along the global path with directly taking into account the kinodynamic limits of the vehicle.

II. Traversability-Anchored Dynamic Path Following (TADPF) Controller

Global free-space connectivity for the vehicle navigation in this navigation scheme is obtained by a global planner. The global navigation function assigns traversability cost values for each free-space position, i.e. some areas are less traversable or even prohibited due to the presence of obstacles. Based on the traversability cost, a measure of cost to a global objective is obtained that takes into account the environment configuration and depends on a specific implementation of the global planner (see further [7] and [8]). By minimizing the cost to goal, the globally optimal geometric path can be obtained.

With the global navigation function available, the aim is to control the vehicle's motion such that it follows the global free-space connectivity based on direct traversability values and/or optimal geometric path computed. The approach of the TADPF controller that was first presented in [10] is recapitulated here, whereas the modifications done in this work are stressed further. The basic concept is in representing the current trajectory of the vehicle, given the low-level control on steering and longitudinal velocity as an arc trajectory, which would be exerted if the commands would be kept constant (see [12] for the first report on this concept). A set of feasible commands given the kinodynamic and

configuration (obstacle) space constraints can be therefore represented as a set of feasible arc trajectories. At each control cycle, the optimal arc (command) can be chosen according to different criteria. Since the presented controller combines both kinodynamically feasible trajectories with the traversability information of the global goal objective it is called "Traversability-Anchored Dynamic Path Following".

A. Kinodynamically feasible vehicle trajectories

The description of the car motion is based on the Ackermann kinematic model:

$$\dot{x} = \cos\theta\, v_l\,, \qquad \dot{y} = \sin\theta v_l\,, \qquad \dot{\theta} = \frac{v_l}{L}\tan\phi\,, \tag{1}$$

with $\{x, y, \theta\}$ being the robot pose and $\{v_l, \phi\}$ the longitudinal velocity and steering angle as control inputs and L the axes distance of the front and rear wheels.

According to the Ackermann kinematics, the vehicle follows a circular path for a given kinematic level control input $\{v_l, \phi\}$. Therefore a set of arc vehicle trajectories can be defined as:

$$\mathcal{A} = \{a_{i,j} = \{x_{i,j}, y_{i,j}\}\,; i = 1 \ldots N_v, j = 1 \ldots N_\kappa\}\ , \tag{2}$$

where N_{v_l} denotes the number of arc sets due to longitudinal velocity $v_{l,i}$ discretization and N_κ the number of arcs due to curvature κ_j discretization, which corresponds to a steering angle ϕ_j.

At each control cycle a trajectory $a_{i,j}$ is chosen, corresponding to a control input $(v_{l,i}, \phi_j)$ that is feasible with respect to the environment constraints, e.g. obstacles and goal direction, but also according to the limitations on the vehicle motion itself. The kinematic limitations on the vehicle motion are the maximum longitudinal velocity $v_{l,max}$, the minimum allowed[1] vehicle speed $v_{l,min}$, and the maximum steering angle ϕ_{max}. The dynamic limitations are the maximum longitudinal acceleration $\dot{v}_{l,max}$ and the maximum steering rate $\dot{\phi}_{max}$. The aim here is to define a minimum set of arcs necessary to take into account the dynamic limitations of the vehicle at each time instant. From Eq. 1 it follows that:

$$\ddot{\theta} = \frac{v_l}{L\cos^2\phi}\dot{\phi} + \frac{\dot{v}_l}{L}\tan\phi\,. \tag{3}$$

Typically, the low-level steering control loop (e.g. power steering) is faster than the longitudinal velocity control loop, thus for small time increments the longitudinal velocity can be considered constant with respect to the angular rate of the vehicle. Therefore, the second term can be neglected in Eq.3. Given that the vehicle is currently on a trajectory defined by $\{v_l, \phi\}$ and the steering rate is at its maximum $\dot{\phi} = \dot{\phi}_{max}$, the curvature change within the kinematic level control sample time-step T_s can be expressed as:

$$\Delta\kappa\,(\phi) = \frac{v_l}{L\cos^2\phi}\dot{\phi}_{max}T_s\,. \tag{4}$$

[1]unless the goal is reached or during an emergency brake

Taking the smallest curvature change within a control cycle T_s such that switching between neighboring arcs is feasible according to steering limitations leads to the a-priori number of arcs due to the curvature discretization:

$$N_\kappa = 2\cdot\lceil\frac{\tan\phi_{max}}{L\,\Delta\kappa\,(\phi_{max})}\rceil + 1\,, \tag{5}$$

taking into account the central $\kappa\,(\phi = 0) = 0$ separately. Moreover, assuming the vehicle drives at its full longitudinal acceleration capability, the number of arc sets due to longitudinal velocity discretization is obtained as:

$$N_{v_l} = \lceil\frac{v_{l,max} - v_{l,min}}{\dot{v}_{l,max}T_s}\rceil\,. \tag{6}$$

B. Configuration space feasible vehicle trajectories - traversability and obstacle cost criteria (Γ_t, Γ_o)

In order to chose an optimal vehicle trajectory-arc at each cycle T_s, an arc that is dynamically feasible is checked for potential collision with obstacles. The global navigation function provides the configuration space obstacle regions. If a prohibited node is encountered along an arc $a_{i,j}$ that is less then break time $T_{b,i} = \frac{v_{l,i}}{\dot{v}_{l,max}}$ away from the starting vehicle position, the arc is banned. For a prediction horizon T_h of vehicle motion along an arc $a_{i,j}$ with length $l(a_{i,j}) = v_{l,i}T_h$, the traversability cost $\Gamma_t^{(i,j)}$ and cost to obstacles $\Gamma_o^{(i,j)}$ are given as:

$$\Gamma_t^{(i,j)} = \sum_{\iota=1}^{N_{t,\iota}} r\left(a_{i,j}^{(\iota)}\right)\quad,\quad \Gamma_o^{(i,j)} = l(a_{i,j}) - l(a_{i,j,o}) \tag{7}$$

where $a_{i,j}^{t}$ corresponds to a sampled point on the arc $a_{i,j}$, $r(\cdot)$ the increment in the navigation function value (traversability and goal directedness cost at that point) and $N_{t,\iota}$ being the number of discrete points up to the traversability prediction horizon $T_t \leq T_h$. The $l(a_{i,j,o})$ represents the length of the arc up to the first occurrence of an obstacle along it, with the condition being $l(a_{i,j,o}) \geq T_{b,i}$, i.e. the arc is still safe according to the dynamic breaking limitations of the vehicle. If an arc is completely void of obstacles then $\Gamma_o^{(i,j)} = 0$. Traversability cost Γ_t gives essentially the global direction of the vehicle to steer to and the obstacle cost slows down the vehicle in presence of close obstacles.

C. Path orientation cost criterion (Γ_r)

In Sec. II-B there was no geometric path to the goal position needed. However, by explicitly computing the path, additional information can be exploited. By following the negative gradient of the global navigation function from the current vehicle position $\{x, y\}$ to the goal $\{g_x, g_y\}$, a global reference path can be constructed that is a set of points $\{c_{r,d} = c_k; k = 1, \ldots, N_g, c_1 = \{x, y\}, c_{N_g} = \{g_x, g_y\}\}$. This path is further smoothed by a spline technique to give a reference path $\mathcal{C}_r(s)$ which is described with the curvilinear parameter s and curve gradient $\|\mathcal{C}_r\,'(s)\| = \sqrt{p'^2(s) + q'^2(s)} \neq 0, \forall s \in [0, s_f]$, where $p(s)$ and $q(s)$ denote the x- and y- component of $\mathcal{C}_r(s)$, respectively.

The kinematic level control objective in this case is to find a longitudinal velocity v_l and steering angle ϕ of the vehicle to follow the reference path $\mathcal{C}_r$ given by the global planner. In particular, a desired reference point is defined on $\mathcal{C}_r(s_d)$ as:

$$x_d = p(s_d)\,,\; y_d = q(s_d)\;,\; (0 \leq s_d \leq s_f)\,. \tag{8}$$

Determining the suitable position of the reference point is important for the path orientation cost of each arc. Here, it is proposed to set the curvilinear length of the reference point proportional to the current longitudinal velocity v_l of the robot with a time prediction horizon T_r (compare with [10]):

$$s_d = T_r v_l \tag{9}$$

and the orientation cost of each arc as:

$$\Gamma_r^{(i,j)} = \frac{\sum_{\iota=1}^{N_{r,\iota}} \|\theta_d - \theta_{i,j}(\iota)\|}{l(a_{i,j,r})} \tag{10}$$

where θ_d is the reference point orientation and $\theta_{i,j}(\iota)$ orientation of the vehicle in the ι-th point along the arc $a_{i,j}$. The cost is scaled to the cumulative length $l(a_{i,j,r}) = v_{l,i}T_r$, with the T_r being the orientation cost prediction horizon.

D. Optimal command choice with comfort criterion

The optimal steering commands $\phi^\star$ chosen at each control cycle minimizes the total weighted sum cost:

$$\phi^\star = \underset{\phi_{i^\star,j}}{\operatorname{argmin}} \left\{ \Gamma^{(i^\star,j)} = \gamma_t \Gamma_t^{(i^\star,j)} + \gamma_g \Gamma_g^{(i^\star,j)} + \gamma \Gamma_o^{(i^\star,j)} \right\}. \tag{11}$$

where each of the costs Γ_t, Γ_o and Γ_r are normalized before weighting. Although the combined cost Γ could be used also for the longitudinal velocity control, it is desired to impose additional constraints on its profile, due to the comfort of the drive, which is related to the maximum lateral acceleration along the path. In the perfect path following case, the vehicle's curvature would be equal to that of the path, so the maximum lateral acceleration for each $v_{l,i}$ is defined as:

$$a_{L,i,max} = \kappa_{max} v_{l,i}^2 \leq a_{L,max} \tag{12}$$

assuming constant movement along the path with curvature κ_{max} on the interval $s \in [0, s_\kappa]$, s_κ being the curvilinear path lookahead. Therefore, the set of feasible longitudinal velocities according to Sec. II-A and Sec. II-A is further constrained to a set of $\tilde{v}_{l,i}$ velocities based on Eq. 12. In order to minimize the travel time, the velocity chosen is:

$$v_l^\star = \max\{\tilde{v}_{l,i}\}\,. \tag{13}$$

III. Sliding Mode Path Following (SMPF) Controller

In [11] a sliding mode controller was developed for path tracking of Ackermann-like vehicles in order to address the issues such as fast response, good transient and robustness with respect to system uncertainties and external disturbances. The path following errors are described by ye and θ_e, where y_e is the lateral distance from the vehicle reference point on the middle of the rear axis $\{x_r, y_r\}$, to the closest point $\{x_d, y_d\}$ on the reference curve $\mathcal{C}_r(s)$, denoted as virtual vehicle position. Angular error θ_e is the difference between the vehicle orientation θ_r and the tangent curve angle at the closest point θ_d, therefore the errors can be written as:

$$\begin{bmatrix} y_e \\ \theta_e \end{bmatrix} = \begin{bmatrix} \cos\theta_d & \sin\theta_d \\ -\sin\theta_d & cos\theta_d \end{bmatrix} \cdot \begin{bmatrix} x_r - x_d \\ y_r - y_d \\ \theta_r - \theta_d \end{bmatrix}. \tag{14}$$

Assuming the kinematics of the vehicle being the same as in Eq. 1, the corresponding error dynamics are:

$$\dot{y}_e = v_l \cdot \sin\theta_e\;,\; \dot{\theta}_e = \dot{\theta}_r = \frac{v_l}{L} tan\phi_r\,, \tag{15}$$

noting that $\dot{\theta}_d = 0$ in the path following problem.

In [11] a sliding surface was proposed which couples together the lateral error y_e and the angular error θ_e:

$$s = \dot{y}_e + k_1 \cdot y_e + k_0 \cdot sgn(y_e) \cdot \theta_e\,. \tag{16}$$

The dynamics of the sliding surface is defined as:

$$\dot{s} = -Q \cdot s - P \cdot sgn(s)\;, \tag{17}$$

where Q and P are scalars such that $Q, P \geq 0$.

The Eq. 16 can also be expressed as:

$$\dot{s} = v_l \cdot \dot{\theta}_e \cos\theta_e + k_1 \cdot v_l \cdot \sin_{\theta_e} + k_0 \cdot sgn(y_e) \cdot \dot{\theta}_e\,. \tag{18}$$

Combining Eq. 15, 17 and 18 yields the desired steering command:

$$\phi_c = \arctan\left(\frac{L}{v_l} \cdot \frac{-Qs - P \cdot sgn(s) - k_1 \cdot v_l \cdot \sin\theta_e}{v_l \cdot \theta_e + k_0 \cdot sgn(y_e)} \right). \tag{19}$$

Note that the longitudinal velocity v_l in this case is not controlled, but is given as an input parameter to the control law of Eq. 19. It may be constant or variable according to a predefined velocity profile along the reference path $\mathcal{C}_r(s)$.

IV. Combined TADPF-SMPF Controller

Although the sliding mode controller of Sec. III provides a fast transient response and small path following error, it has two basic disadvantages. Firstly, it does not take explicitly into account the constraints on the control inputs, such as maximal steering angle ϕ_{max}, nor the dynamic constraints $\dot{v}_{l,max}$ and $\dot{\phi}_{max}$ as described in Sec. II-A.

Secondly, there is no check for collision of the chosen vehicle trajectory arising from a given control input ϕ_c at v_l, as is done for the TADPF controller in Sec. II-B. This effectively means that the vehicle may hit an obstacle or end in other potentially hazardous situation if there is a significant deviation from the pre-planned reference path, due to path following error, external disturbances or other non-modeled effects.

In order to resolve both these aspects and render the navigation of the vehicle safe while taking into account the control and dynamic limitations of the vehicle, the proposed new controller combines both TADPF and SMPF strategies.

The longitudinal velocity $v_l^\star$ is given by Eq. 13 along the global path and the steering command ϕ_c is given by the SMPF controller of Eq. 19. In order to enforce the constraints of Sec. II-A and Sec. II-B, the steering command at each instant is calculated as:

$$\phi_c^\star = \underset{\phi_{c,j}}{\operatorname{argmin}} \{\|\phi_{c,j} - \phi_c\|\} \ . \tag{20}$$

Thus, the optimal control chosen is defined by the arc of the TADPF controller $\{v_l^\star, \phi_c^\star\}$ that is also checked to be configuration space feasible and matches the closest the input command given by the SMPF control strategy $\{v_l, \phi_c\}$, resulting in the TADPF-SMPF control strategy.

V. RESULTS

A. TADPF controller

The path following schemes were tested in a simulation environment based on "Sunflower Mobile Robot Library", which is a framework of classes and utilities for mobile robotics, particularly an implementation of path planning and obstacle avoidance ([13]). The vehicle scenario was to travel through a set of goal positions while avoiding any obstacles on the way. A lidar sensor is attached to the vehicle scanning in the frontal horizontal plane with limited range. As new environment information is available, the global navigation function is recomputed by wavefront expansion from the current goal position. Based on the gradient information from the navigation function, a globally feasible path for the vehicle to follow is available on-line from any position in the free configuration space. The left side of Fig. 1 shows the global view of a situation where the vehicle approaches a goal position and the wayfront is expanded in order to account for newly available obstacle information given by the lidar. On the right of Fig. 1, a zoom-in on the vehicle and currently feasible trajectories (arcs) is given. Free trajectories are marked green, the ones that hit obstacles but are still valid according to the dynamic breaking distance of the vehicle (shown on each arc with corresponding color points) are given in red and the trajectories along the re-propagating wayfront are given in magenta. In the re-propagation (replanning) period the global gradient is not available, however, the traversability information (obstacles) is updated at all times, ensuring safety. The reference point position on the path is given in green.

Fig. 2 and 3 show the trajectory and steering comparison between different versions of the TADPF controllers where only traversability-obstacle cost is taken into account (Γ_t, Γ_o) versus reference path orientation cost controller (Γ_r) and the full controller with all three costs, when the vehicle is driven at a constant speed of $v_l = 20km/h$. As can be seen, both separate cost options give similar steering controls. The combined cost pattern depends on the weighting factors of each contribution, where a balanced weighting gives a smoothing effect on the net steering and trajectory.

In the next test drive, the vehicle was allowed to drive the speeds from $v_{l,min} = 10km/h$ up to $v_{l,max} = 30km/h$. When analyzing the longitudinal velocity of the traversability-obstacle cost in Fig. 4, it can be seen that the speed is maximized due to the max. traversability change criteria (Eq. 7) with the longest arc distance. Slowing down is performed at times only due to the obstacle cost component. Although the safety criteria are thus satisfied, the Fig. 7 shows extremely high lateral accelerations up to $a_L = 12m/s^2$, which is clearly inacceptable. By taking the lateral acceleration constraints into account from Eq. 12, the maximal v_l along the path can be limited as is shown for the case of the orientation cost profile, where maximum speeds attained are lower (see Fig. 5) but the lateral acceleration a_L is drastically decreased. On average, the a_L stays well withing the bounds $a_{L,max} = 1m/s^2$ for fairly comfortable driving ([14]) as in Fig. 8. The peak values of up to $a_L = 2.5m/s^2$ are due to abrupt change of path orientation and curvature beyond a goal waypoint, when a completely new path is replanned to the next goal. This situation can be improved by parallel planning of the next goal path, while the current one is still being executed and jointed to the next one smoothly at the current goal position, which is the topic of future work. Fig. 6 shows the reference point position ρ which increases proportional to the longitudinal speed. Fig. 9 shows the current vehicle curvature and that of the closest point along the path for the vehicle and the reference point itself. In the perfect tracking case, the vehicle should have the same curvature as the reference point with a time delay related to the vehicle speed. Main differences can be observed due to initial misalignment of the vehicle orientation with respect to the path and the holonomicity of the path itself. Since the path is generated on-line and the vehicle motion is guaranteed to be safe due to the collision checks along currently chosen command/trajectory, small path following errors are acceptable. The velocity profile of Fig. 5 has a quality of a time-optimal profile, in the sense that the vehicle is always driving with the maximum allowed speed according to the safety and comfort measure on lateral acceleration. A further improvement is forseen in generating a smoother profile where the vehicle might take a longer time to traverse a given path but with less acceleration-deceleration phases.

B. TADPF-SMPF controller

This section deals with comparison of the TADPF and the SMPD controller and their combined version as given in Fig. 10 to Fig. 14. Since the SMPF control scheme does not provide longitudinal velocity commands, the lateral acceleration based constraints along the path of the TADPF control scheme (Eq. 12 and Eq. 13) were used to generate the longitudinal velocity control inputs in all three cases (Fig. 10). When analyzing the steering angle, curvature and lateral acceleration of the vehicle in the Fig. 11, 12 and 13, respectively, it can be seen that the peak values of the TADPF method are smaller, due to the fact that a reference point look-ahead distance is used, combined with the global navigation function in the configuration space. On the other hand, the SMPF and TADPF-SMPF rely exclusively on the vehicle reference point, which is effectively the closest point

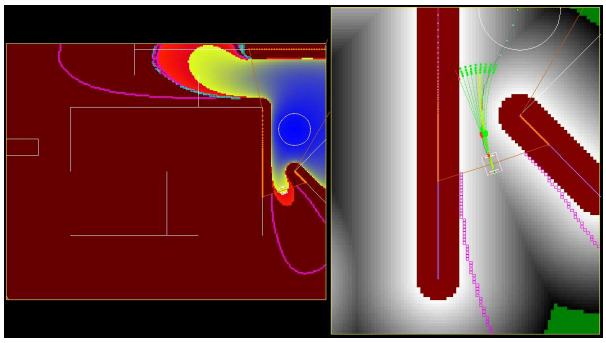

Fig. 1. Global environment snapshot with local trajectory view

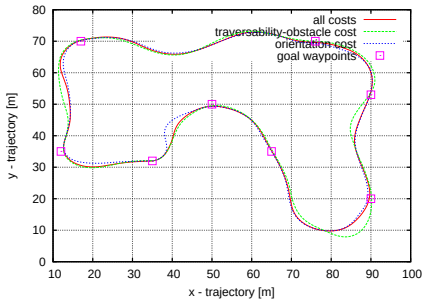

Fig. 2. Trajectory x-y comparison for TADPF

on the path with respect to the vehicle rear-axes middle point. As a consequence, abrupt changes in path curvature and tangent direction may cause steering angle control peaks. However, The TADPF-SMPF method provides smaller path following errors with respect to the path generated by the global planner and can be used efficiently and with less control effort if the global path is smooth enough. In comparison, the TADPF method alone tends to smoothen the vehicle trajectory through the free space because it's based on both global navigation function and current trajectory as can be seen in Fig. 14.

If the smoothness and non-holonomicity of the on-line generated global path is not guaranteed, the TADPF method alone is preferred, since it produces less steering signal effort, while still following the global path direction. In contrast, if a global path is smooth, possibly optimized for lesser curvature change along the whole path, the preferred method is TADPF-SMPF that provides smaller path following errors and is invariant on the choice of the reference point lookahead distance, since it is bound to the closest point on the path. Note that the SMPF controller alone is not suitable for real application, since it provides no guarantees on safety with comparison to TADPF or TADPF-SMPF method, which include collision checks at each cycle. Moreover, the dynamic constraints are not taken into account, which can cause larger delays or even instabilities in the cases of limited actuators, in this case particularly the steering rate $\dot{\phi}$.

Both TADPF and TADPF-SMPF control methods have been tested extensively experimentally on the Smart test vehicle at constant longitudinal speeds of up to $20km/h$, see [15] and [16], respectively.

VI. Conclusion and Outlook

In this work, three different control strategies to path following for autonomous navigation of vehicles have been analyzed and compared. Firstly, the TADPF controller is based on a set of feasible arc trajectories according to kinodynamic and configuration space constraints, where the optimal command is chosen according to the global objective along the path. Longitudinal velocity profile was determined in this paper according to the lateral acceleration constraints for increased comfort of driving. A control theory based SMPF controller was analyzed and enhanced with the obstacle collision avoidance, kinodynamic and comfort limits of the vehicle at each control cycle, resulting in the TADPF-SMPF control scheme. Thus, inherent safety and account for vehicle dynamic limits was achieved, regardless of the specific path following scheme used. The TADPF control scheme provided less steering control effort due to the usage of the global navigation function smoothing of free-space, whereas TADPF-SMPF control scheme provided less path following error with the expense of increased steering effort. In future work, both TADPF and TADPF-SMPF controllers will be tested also on a global path that will be further optimized after the initial smoothed geometric path of the global navigation function is obtained. It is expected that decreasing the curvature changes along the global path will also decrease the steering control effort of the vehicle. Furthermore, a longitudinal velocity profile could be introduced with less acceleration-deceleration phases based on multi-step velocity prediction along the path in comparison to the one-step velocity prediction in the current scheme.

VII. Acknowledgments

This work has partly been supported by the EC under contract number FP6-IST-027140-BACS.

References

[1] A. Kelly and A. Stentz, "Rough terrain autonomous mobility - part 2: An active vision, predictive control approach," *Autonomous Robots*, vol. 5, pp. 163–198, 1998.

[2] M.L.E. Aguilar, P. Soueres, M. Courdesses, and S. Fleury, "Robust path-following control with exponential stability for mobile robots," in *Proc. of the IEEE ICRA*, 1998.

[3] C. Samson, "Control of chained systems. application to path following and time-varying point-stabilization of mobile robots," *IEEE Trans. on Automatic Control*, vol. 40, no. 1, pp. 64–77, 1995.

[4] E. Red, "A dynamic optimal trajectory generator for cartesian path following," *Robotica*, vol. 18, pp. 451–458, 2000.

[5] F. Lamiraux and J.-P. Laumond, "Flatness and small-time controllability of multibody mobile robots: Application to motion planning," *IEEE Trans. on Automatic Control*, vol. 45, pp. 1878–1881, 2000.

[6] C. Coelho and U. Nunes, "Path-following control of mobile robots in presence of uncertainties," *IEEE Trans. on Robotics*, vol. 21, no. 2, pp. 252–261, 2005.

[7] R. Philippsen and R. Siegwart, "An interpolated dynamic navigation function," in *Proc. of the IEEE ICRA*, 2005.

[8] D. Ferguson and A. Stentz, "Field D*: An interpolation-based path planner and replanner," in *Proc. of the Int. Symposium on Robotics Research (ISRR)*, 2005.

[9] K. Macek, I. Petrovic, and R. Siegwart, "A control method for stable and smooth path following of mobile robots," in *Proc. of the European Conference on Mobile Robots (ECMR)*, 2005.

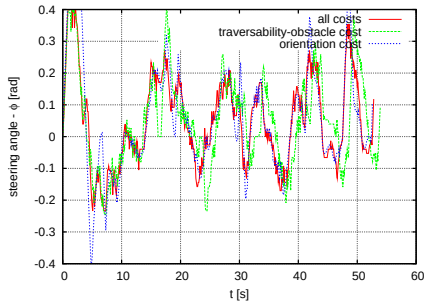

Fig. 3. Steering angle ϕ comparison for TADPF

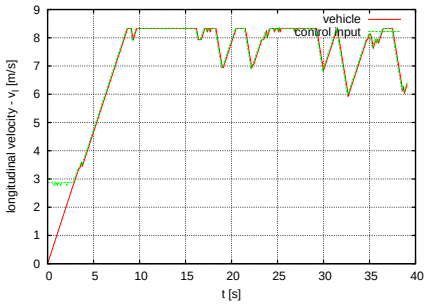

Fig. 4. Velocity v_l for TADPF with Γ_t and Γ_o

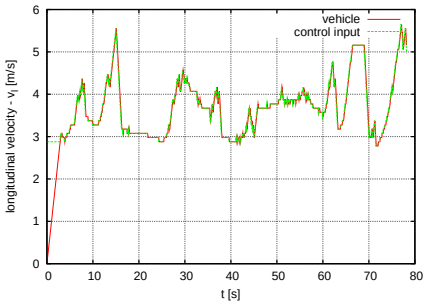

Fig. 5. Velocity v_l for TADPF with Γ_r

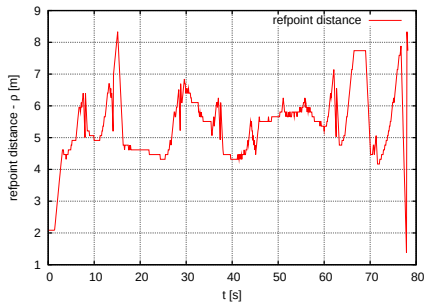

Fig. 6. Refpoint distance ρ for TADPF with Γ_r

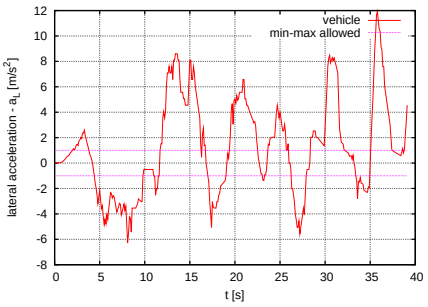

Fig. 7. Lateral acceleration a_L for TADPF with Γ_t and Γ_o

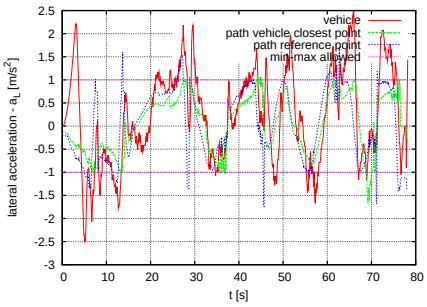

Fig. 8. Lateral acceleration a_L for TADPF with Γ_r

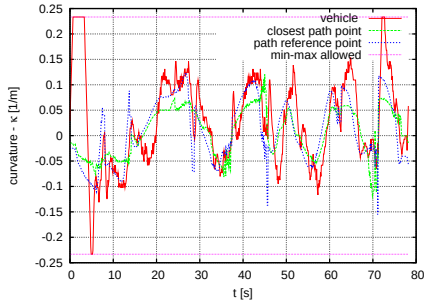

Fig. 9. Curvature κ for TADPF with Γ_r

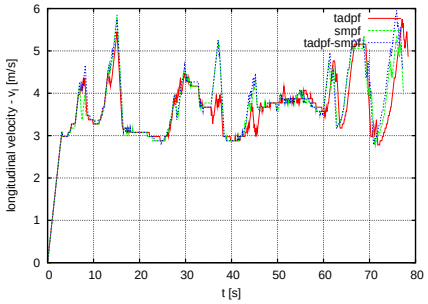

Fig. 10. Velocity v_l comparison for all controllers

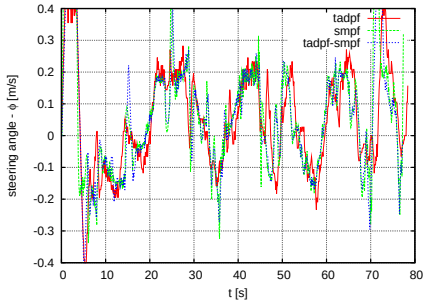

Fig. 11. Steering angle ϕ comparison for all controllers

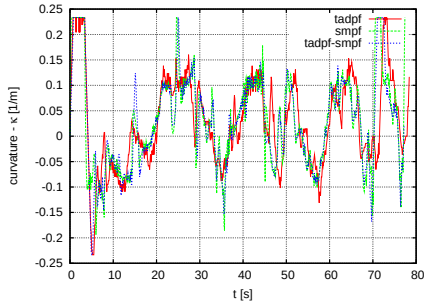

Fig. 12. Curvature κ comparison for all controllers

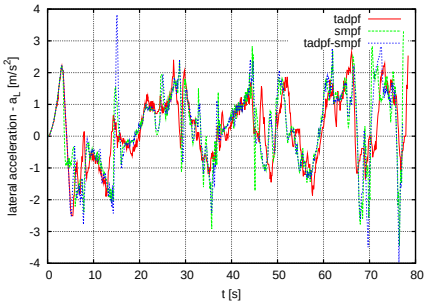

Fig. 13. Lateral acceleration a_L comparison for all controllers

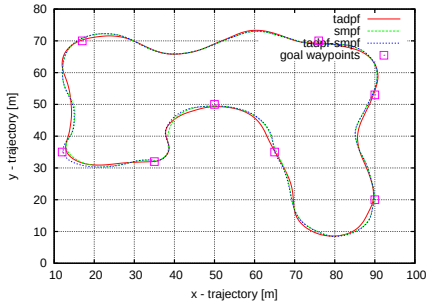

Fig. 14. Trajectory x-y comparison for all controllers

[10] Jur van den Berg, Dave Ferguson, and James Kuffner, "Path planning, replanning and execution for autonomous driving in urban and offroad environments," in *IEEE Int. Conference on Robotics and Automation (ICRA) Workshop on Planning, Perception and Navigation of Intelligent Vehicles (PPNIV)*, 2007.

[11] R. Solea and U. Nunes, "Trajectory planning with velocity planner for fully-automated passenger vehicles," in *Proc. of the IEEE Intelligent Transportation Systems Conference (ITSC)*, 2006.

[12] D. Fox, W. Burgard, and S. Thrun, "Controlling synchro-drive robots with the dynamic window approach to collision avoidance," in *Proc. of the IEEE/RSJ Int. Conference on Intelligent Robots and Systems (IROS)*, 1996.

[13] *"http://sourceforge.net/projects/libsunflower"*.

[14] *ISO, Mechanical vibration and shock-Evaluation of human exposure to whole body vibrations: P1: General requirements, ISO 2631-1*, 1997.

[15] *"https://lsa1pc12.ethz.ch/svn/kristijan/public/videos/tadpf.mpg"*.

[16] *"https://lsa1pc12.ethz.ch/svn/kristijan/public/videos/tadpf-smpf.mpg"*.